Itinerant ferromagnetism by e_g and t_{2g} states in the two-band Hubbard model

2009 J. Phys.: Condens. Matter 21 035601

(http://iopscience.iop.org/0953-8984/21/3/035601)

J. Phys.: Condens. Matter **21** (2009) 035601 (5pp) doi:10.1088/0953-8984/21/3/035601

Itinerant ferromagnetism by e_g and t_{2g} states in the two-band Hubbard model

Nozomu Kamakura

Institute of Materials Structure Science, KEK, 1-1 Oho, Tsukuba, Ibaraki 305-0801, Japan

E-mail: nozomu.kamakura@kek.jp

Received 6 July 2008, in final form 13 October 2008
Published 11 December 2008
Online at stacks.iop.org/JPhysCM/21/035601

Abstract

Itinerant ferromagnetism derived from e_g and t_{2g} states has been studied by the Gutzwiller variational method based on the two-band Hubbard model. The analysis shows that the magnetization value that depends on the orbital reflects strength of renormalization for each band. As a result, the magnetization of the 3d(t_{2g}) band, which is more strongly renormalized in the calculation, has a larger value than that of the 3d(e_g) band. By changing the atomic interaction and projected orbital density of states (DOS), we have discussed general tendencies that the magnetizations by the e_g and t_{2g} states are determined by the relative intensities of the projected orbital DOS at the Fermi energy, the renormalized kinetic energies relative to U, and stability of atomic multielectron configuration states. The result indicates that increases in Coulomb interaction U and the portion of Hund's coupling J in the atomic interaction lead to balanced magnetizations between the two states. Variation in the above factors can generate a variety of spin-dependent electronic structures near the Fermi energy in 3d transition metal ferromagnets.

1. Introduction

The correlation effect on itinerant ferromagnetism of 3d transition metals has been extensively studied so far. Theories beyond the Stoner approximation [1] have shown a qualitatively consistent correlation effect [2–4] that stabilization of the ferromagnetic state requires larger interaction than the expectation based on single-particle theory. In addition to the correlation for a single band, the importance of band degeneration has been suggested for understanding of the itinerant ferromagnetism. In [5], the Gutzwiller method has been generalized to the multi-band Hubbard model with general on-site Coulomb interactions. As a specific application of this scheme, characteristics of itinerant ferromagnetism by two degenerate e_g orbitals, which have identical projected orbital DOS, were investigated [5]. There, effects of the band degeneration on the magnetic properties such as the magnetization as a function of the atomic interaction and the role of Hund's coupling in them were examined. On electronic states, the correlation effect brings a narrowing of bandwidth and exchange splitting. In particular, this effect on 3d band structure has been studied in ferromagnetic nickel, experimentally and theoretically [6–12]. As a result, description of quasi-particle band structure has been markedly improved by band theory considering the correlation effect such as the GW approximation (GWA) combined with dynamical mean-field theory (DMFT) [10] and the generalized Hubbard model based on the Gutzwiller approximation [11].

Here, we address the issue relating to characteristics of 3d transition metal ferromagnets that both the 3d(e_g) band and 3d(t_{2g}) band form the Fermi surface and contribute to the magnetism. In the case of ferromagnetic nickel, it has been observed as a difference between the magnetizations derived from the e_g and t_{2g} states and has been thought to relate to conflicting parts in the band structure near the Fermi energy. For example, there has been discrepancy in the existence of the hole pocket by the X_2 minority spin band. The hole pocket by the minority spin band of X_2 (e_g) and its relation to the area of the Fermi surface by the minority spin band of X_5 (t_{2g}) are determined by anisotropy of the exchange splitting. Several experimental results have indicated a large anisotropy (a factor of about two) in the exchange splitting between the e_g and t_{2g} states and disappearance of the X_2 minority spin hole pocket [9, 11], contrary to band structure calculations such as local density approximation (LDA) calculations [6]. Experimental results indicating the existence of the X_2 minority spin hole pocket have also been reported [12]. The magnetizations by the e_g and t_{2g} states, which have different values, connect with the anisotropy of the exchange splitting via the DOS. Interaction between the

e_g and t_{2g} orbitals can relate to the difference between the magnetizations by these states. On the basis of the above situation, we investigate the correlation effect on e_g and t_{2g} electrons by the multi-band model and the magnetizations derived from the e_g and t_{2g} states. For this analysis, we have applied the Gutzwiller variational method to the two-band Hubbard model consisting of the e_g and t_{2g} states on a face centred cubic (fcc) lattice. By applying the expression of the generalized Gutzwiller method in [5] to the model system consisting of the two states that have different projected orbital DOSs, the explicit form of the renormalization factor and the variational energy is obtained for this specific case. Using the obtained expression, the magnetizations derived from the e_g and t_{2g} states are analysed as functions of atomic interactions, and the difference (or ratio) between the magnetizations of the two states is studied. The simplification into the two bands allows one to fully examine the magnetic behaviour of these states by changing the atomic interaction and the DOS, which vary among ferromagnetic 3d transition metals Fe, Co, and Ni. The lattice parameter, dimensionality, and surface–bulk feature would also affect them. Therefore, although the calculation is performed with an ideal model, it may help us to understand characteristics of spin-dependent band structures and ferromagnetism of 3d transition metals.

2. Model and method

The Hamiltonian of the two-band Hubbard model $\hat{H}$ is written in terms of the single-particle part $\hat{H}_1$ and the atomic part $\hat{H}_{\rm at}$:

$$\begin{aligned}\hat{H} &= \sum_{i,j;\boldsymbol{\sigma},\boldsymbol{\sigma}'} t_{i,j}^{\boldsymbol{\sigma},\boldsymbol{\sigma}'} \hat{c}^{\dagger}_{i;\boldsymbol{\sigma}} \hat{c}_{j;\boldsymbol{\sigma}'} + \sum_i \hat{H}_{i;\rm at} = \hat{H}_1 + \hat{H}_{\rm at},\\ \hat{H}_{i;\rm at} &= U \sum_b \hat{n}_{b,\uparrow}\hat{n}_{b,\downarrow} + U' \sum_{\sigma,\sigma'} \hat{n}_{{\rm e_g},\sigma}\hat{n}_{{\rm t_{2g}},\sigma'}\\ &\quad - J \sum_{\sigma} \hat{n}_{{\rm e_g},\sigma}\hat{n}_{{\rm t_{2g}},\sigma} + J \sum_{\sigma} \hat{c}^{\dagger}_{{\rm e_g},\sigma}\hat{c}^{\dagger}_{{\rm t_{2g}},-\sigma}\hat{c}_{{\rm e_g},-\sigma}\hat{c}_{{\rm t_{2g}},\sigma}\\ &\quad + J(\hat{c}^{\dagger}_{{\rm e_g},\uparrow}\hat{c}^{\dagger}_{{\rm e_g},\downarrow}\hat{c}_{{\rm t_{2g}},\downarrow}\hat{c}_{{\rm t_{2g}},\uparrow} + \hat{c}^{\dagger}_{{\rm t_{2g}},\uparrow}\hat{c}^{\dagger}_{{\rm t_{2g}},\downarrow}\hat{c}_{{\rm e_g},\downarrow}\hat{c}_{{\rm e_g},\uparrow}),\end{aligned} \tag{1}$$

where $\hat{c}^{\dagger}_{i;\boldsymbol{\sigma}}$ in $\hat{H}_1$ creates an electron with combined spin–orbit index $\boldsymbol{\sigma}$ at the lattice site i. In this study, we have used two 3d orbitals, $\mathrm{d}(x^2-y^2)$ (e_g) and $\mathrm{d}(zx)$ (t_{2g}). In $\hat{H}_{\rm at}$, the specific form for the e_g and t_{2g} orbitals with spin σ is used, U (U') denotes the intra- (inter-) orbital Coulomb interaction and J is the Hund's coupling. The orbitals $\mathrm{d}(x^2-y^2)$ and $\mathrm{d}(zx)$ are labelled as $b=1$ and 2, respectively. Among the interactions in $\hat{H}_{\rm at}$, the relation $U-U'=2J$ that comes from the cubic symmetry holds. The general formulation for the Gutzwiller method based on the multi-band Hubbard model is given in [5]. In figure 1, notation for the probabilities of the multielectron configuration states and the energies of the atomic configurations obtained from $\hat{H}_{\rm at}$ are shown for the present case. The projected orbital DOS is obtained using tight-binding Hamiltonian $\hat{H}_1$ with first- and second-nearest-neighbour hopping matrix elements as described in [13]. The model calculations by the Gutzwiller method are performed using the DOS obtained from two hopping parameter sets, which are set as examples of itinerant electron systems. The hopping parameters for DOS1 are set at $(t_{dd\sigma})_1 = 0.5$ eV, $(t_{dd\sigma})_2 = 0.04$ eV, and $t_{dd\sigma}$:$t_{dd\pi}$:$t_{dd\delta}$ = 1.0:(−0.6):0.1. Those for DOS2 are $(t_{dd\sigma})_1 = 0.5$ eV, $(t_{dd\sigma})_2 = 0.08$ eV, and $t_{dd\sigma}$:$t_{dd\pi}$:$t_{dd\delta}$ = 1.0:(−0.6):0.1. Thus, DOS1 and DOS2 collectively indicate the DOS set, including the total DOS ($D_0(\epsilon)$), and the DOS projected onto the e_g orbital ($D_{{\rm e_g},0}(\epsilon)$) and t_{2g} orbital ($D_{{\rm t_{2g}},0}(\epsilon)$) by each hopping parameter set. In figure 2, $D_0(\epsilon)$ ($=D_{{\rm e_g},0}(\epsilon)+D_{{\rm t_{2g}},0}(\epsilon)$), $D_{{\rm e_g},0}(\epsilon)$ and $D_{{\rm t_{2g}},0}(\epsilon)$, which are the calculated results per site and per spin, are shown for DOS1 and DOS2. As shown later, calculations by the peak of DOS1 and DOS2 give ferromagnetic solutions by typical potential parameters in correlated electron systems. In figure 2, the difference between DOS1 and DOS2 is prominent especially in the relative intensity of the DOS projected onto the two orbitals at the Fermi energy. The calculations with two kinds of DOS set are performed to examine the magnetic behaviour with such a difference of DOS shape. In the case treating the e_g and t_{2g} orbitals, the renormalization factor $q_{b,\sigma}$ (<1) for orbital b and spin σ is described by the probabilities and electron occupation $n^0_{b,\sigma}$:

$$\begin{aligned}q_{b=i_b,\sigma} &= \frac{1}{n^0_{b=i_b,\sigma}(1-n^0_{b=i_b,\sigma})}\\ &\quad\times\Big[(\sqrt{s_{b=i_b,-\sigma}}+\sqrt{t_{b=i_b,\sigma}})\tfrac{1}{2}(\sqrt{d_{\rm E}}+\sqrt{d_{\rm A}})\\ &\quad+(\sqrt{s_{b=j_b,-\sigma}}+\sqrt{t_{b=j_b,\sigma}})\tfrac{1}{2}(\sqrt{d^0_{\rm t}}+\sqrt{d_{\rm s}})+\sqrt{e}\sqrt{s_{b=i_b,\sigma}}\end{aligned}$$

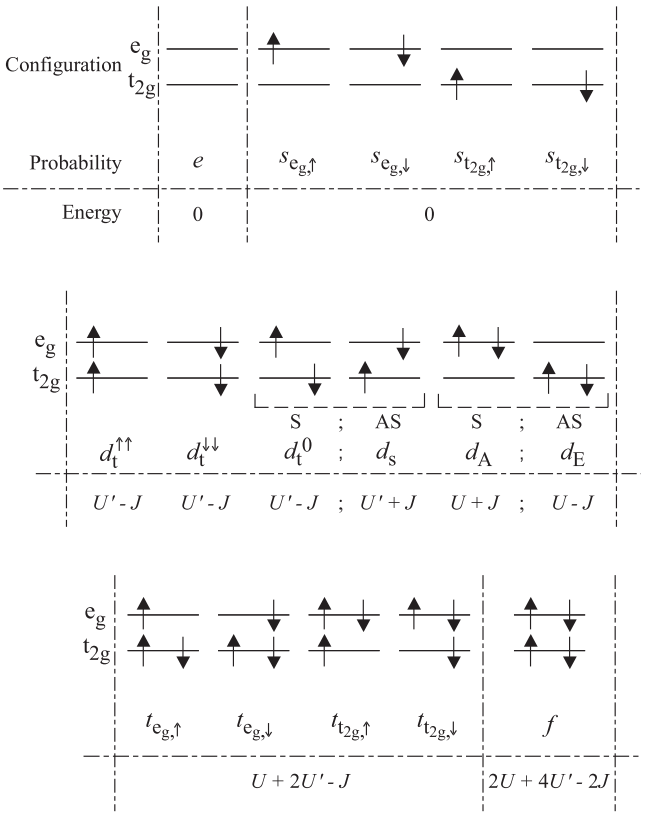

Figure 1. Configurations show the eigenstates of $\hat{H}_{\rm at}$, while S and AS indicate that the symmetric and antisymmetric combinations of the designated configurations are the eigenstates of $\hat{H}_{\rm at}$, respectively. Notations for the probabilities and energies of the eigenstates are also indicated.

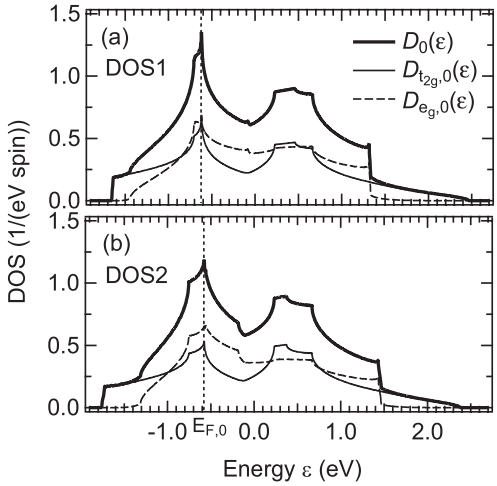

Figure 2. The DOSs projected onto the e_g orbital ($D_{e_g,0}(\epsilon)$) and t_{2g} orbital ($D_{t_{2g},0}(\epsilon)$) are shown by broken and solid lines, respectively. The total DOS $D_0(\epsilon)$ is shown by a thick solid line. (a) and (b) show the results for DOS1 and DOS2, respectively. The vertical broken lines indicate $E_{F,0}$, which is the Fermi energy initially set before the calculation of the magnetization.

$$+\sqrt{s_{b=j_b,\sigma}}\sqrt{d_t^{\sigma\sigma}}+\sqrt{d_t^{-\sigma-\sigma}}\sqrt{t_{b=j_b,-\sigma}}+\sqrt{t_{b=i_b,-\sigma}}\sqrt{f}\Big]^2, \quad (2)$$

where i_b, $j_b = 1$ or 2, and $i_b \neq j_b$. The occupation $n^0_{b,\sigma}$ to the DOS projected onto orbital b with spin σ is written as $n^0_{b,\sigma} = \int_{-\infty}^{E_{F,b,\sigma}} d\epsilon\ D_{b,0}(\epsilon)$. Here, $E_{F,b,\sigma}$ indicates the Fermi energy for orbital b with spin σ. Also notation for the probabilities in figure 1 is used in the equation. The symbol $s_{b=i_b,\sigma}$ denotes the probability for a single occupancy of orbital $b = i_b$ with spin σ. The probability for a triple occupancy of orbital $b = i_b$ with spin σ and orbital $b = j_b$ with both spins is indicated by $t_{b=i_b,\sigma}$. The symbols $d_t^{\uparrow\uparrow}$, $d_t^{\downarrow\downarrow}$, d_t^0, d_s, d_E, and d_A represent the probabilities to find doubly occupied states $|\uparrow,\uparrow\rangle$, $|\downarrow,\downarrow\rangle$, $(|\uparrow,\downarrow\rangle + |\downarrow,\uparrow\rangle)/\sqrt{2}$, $(|\uparrow,\downarrow\rangle - |\downarrow,\uparrow\rangle)/\sqrt{2}$, $(|\uparrow\downarrow,0\rangle - |0,\uparrow\downarrow\rangle)/\sqrt{2}$, and $(|\uparrow\downarrow,0\rangle + |0,\uparrow\downarrow\rangle)/\sqrt{2}$, respectively. The probabilities for empty and fully occupied sites are indicated by e and f. The variational energy $E^{\rm var}$ consists of the kinetic energy part and atomic interaction part (equation (3)). The kinetic energy part (renormalized kinetic energy) for orbital b with spin σ is given by the product of the kinetic energy $\bar{\epsilon}_{b,\sigma,0}$ of the electron in the uncorrelated state and the renormalization factor $q_{b,\sigma}$. Here, $\bar{\epsilon}_{b,\sigma,0}$ is given by $\bar{\epsilon}_{b,\sigma,0} = \int_{-\infty}^{E_{F,b,\sigma}} d\epsilon\ \epsilon D_{b,0}(\epsilon)$. Then, the variational energy $E^{\rm var}$ for the present case is written as

$$\begin{aligned}E^{\rm var} &= \sum_\sigma q_{e_g,\sigma}\bar{\epsilon}_{e_g,\sigma,0} + \sum_\sigma q_{t_{2g},\sigma}\bar{\epsilon}_{t_{2g},\sigma,0}\\ &+ (U'-J)(d_t^{\uparrow\uparrow}+d_t^0+d_t^{\downarrow\downarrow})\\ &+ (U'+J)d_s + (U'+J)d_E\\ &+ (U+J)d_A + (U+2U'-J)\\ &\times (t_{e_g,\uparrow}+t_{e_g,\downarrow}+t_{t_{2g},\uparrow}+t_{t_{2g},\downarrow})\\ &+ (2U+4U'-2J)f. \end{aligned} \quad (3)$$

The magnetizations by the e_g and t_{2g} states are determined so as to minimize $E^{\rm var}$. Here, the magnetization derived from orbital b is $M(b) = (n^0_{b,\uparrow} - n^0_{b,\downarrow})/2$. The probabilities for a singly occupied site and an empty site are described by

$$\begin{aligned}s_{b=i_b,\sigma} &= n^0_{b=i_b,\sigma} - [d_t^{\sigma\sigma} + \tfrac{1}{2}(d_t^0 + d_s + d_E + d_A)\\ &+ t_{b=i_b,\sigma} + t_{b=j_b,\sigma} + t_{b=j_b,-\sigma} + f], \end{aligned} \quad (4)$$

where $i_b \neq j_b$, and

$$\begin{aligned}e &= 1 - n^0_{e_g,\uparrow} - n^0_{e_g,\downarrow} - n^0_{t_{2g},\uparrow} - n^0_{t_{2g},\downarrow} + d_t^{\uparrow\uparrow} + d_t^0 + d_t^{\downarrow\downarrow}\\ &+ d_s + d_E + d_A + 2t_{e_g,\uparrow} + 2t_{e_g,\downarrow} + 2t_{t_{2g},\uparrow} + 2t_{t_{2g},\downarrow} + 3f, \end{aligned} \quad (5)$$

respectively. These give relations between probabilities and electron occupations, and provide restriction in the minimization problem.

3. Results and discussion

First, the calculation by the Gutzwiller method is performed using the orbital-averaged DOS ($D_0(\epsilon)/2$). Thus, the two orbitals are set to have identical average DOS, which formally corresponds to the calculation by doubly degenerate orbitals. The obtained magnetization is shown in figures 3(a) and (b), in which U' and J are set at $0.6U$ and $0.2U$, respectively. Since the calculation is performed by initially setting the occupancy that corresponds to the DOS peak at the Fermi energy $E_{F,0}$ ($n_0 = 0.27$ and 0.29 for DOS1 and DOS2, respectively), the ferromagnetic state occurs from $U \sim 2.5$ eV and 3.0 eV in figures 3(a) and (b), respectively. Here, n_0 and $E_{F,0}$ denote the occupation of $D_0(\epsilon)/2$ and Fermi energy that are initially set before the minimization process of the variational energy, respectively. Thus, n_0 is given by $n_0 = (1/2)\int_{-\infty}^{E_{F,0}} d\epsilon D_0(\epsilon)$. If the Gutzwiller method is performed by the DOS projected onto the e_g orbital ($D_{e_g,0}(\epsilon)$) and t_{2g} orbital ($D_{t_{2g},0}(\epsilon)$), different magnetization values are obtained for the two states, reflecting the difference in the projected orbital DOS. The result is also shown in figures 3(a) and (b), in which the magnetization of the t_{2g} states has larger value than that of the e_g states. Since the spin-averaged kinetic energy $\bar{\epsilon}_{b,0}$ ($=(\bar{\epsilon}_{b,\uparrow,0} + \bar{\epsilon}_{b,\downarrow,0})/2$) of the electron in the uncorrelated state has larger absolute value, with the negative sign for the $3d(t_{2g})$ band with wider bandwidth, the renormalization factor for the t_{2g} states has smaller value than that for the e_g states in the minimum of $E^{\rm var}$. For example, by using DOS1, the spin-averaged renormalization factor $q_b(=(q_{b,\uparrow} + q_{b,\downarrow})/2)$ is 0.806 and 0.710 for the $3d(e_g)$ and $3d(t_{2g})$ bands, respectively, with the atomic interaction $U = 4.0$ eV ($U' = 0.6U$ and $J = 0.2U$). The $q_{t_{2g}}$ factor is actually smaller than the q_{e_g} factor. As a result, the $3d(t_{2g})$ band is renormalized more strongly and causes band narrowing, leading to larger magnetization of the t_{2g} states. The orbital-averaged magnetization deviates from the middle of the magnetizations of the two states, which indicates the importance of analysis using the multi-band model for determination of the total magnetization.

Although the magnetizations of the e_g and t_{2g} states are found to be strongly affected by the strength of the renormalization that reflects the value of $\bar{\epsilon}_{b,0}$ in the minimization of $E^{\rm var}$ (equation (3)), the detailed magnetization value should depend on the projected orbital DOS at $E_{F,0}$,

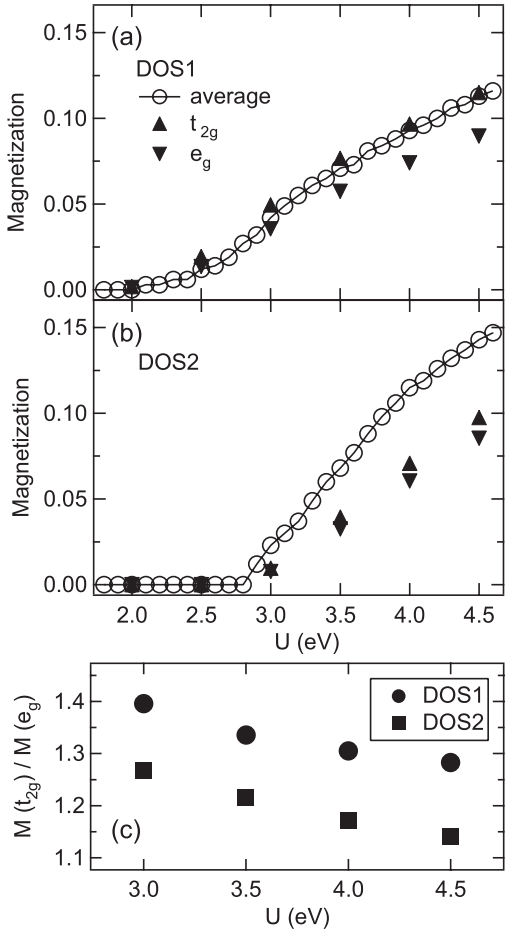

Figure 3. (a) and (b) magnetization by the orbital-averaged DOS is plotted as a function of U by open circles. The results using DOS1 and DOS2 are shown in (a) and (b), respectively. Orbital-dependent magnetizations of the e_g and t_{2g} states using their projected orbital DOS are shown by down and up triangles, respectively. In the calculation, U' and J are set at $0.6U$ and $0.2U$, respectively. (c) The magnetization of the t_{2g} states relative to that of the e_g states ($M(t_{2g})/M(e_g)$) is shown. The results by DOS1 and DOS2 are indicated by the circle and square, respectively.

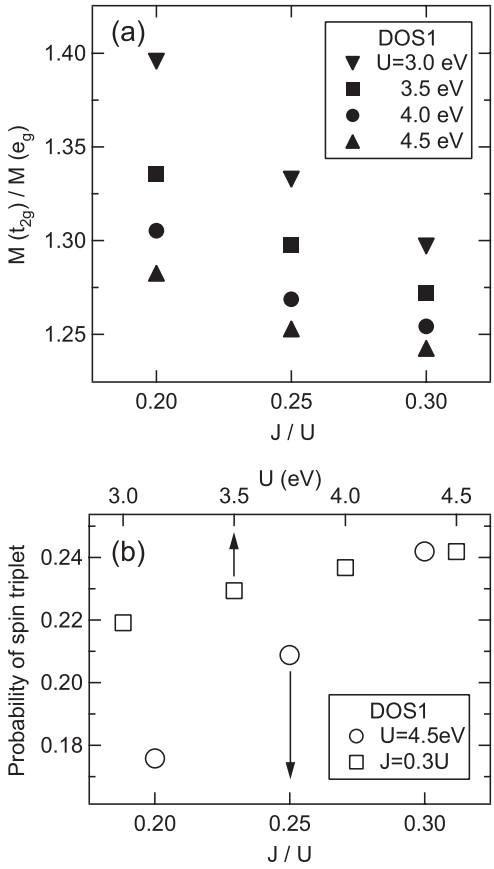

Figure 4. (a) $M(t_{2g})/M(e_g)$ is calculated as a function of the portion of J by using DOS1. (b) The probability of the spin triplet states (the sum of $d_t^{\uparrow\uparrow}$, $d_t^{\downarrow\downarrow}$, and d_t^0) calculated by using DOS1. The calculation as a function of the portion of J (bottom axis) is performed at $U = 4.5$ eV (circle). In the result as a function of U (top axis), $J(U')$ is set at $0.3U$ ($0.4U$) (square).

which can significantly influence the ratio between the magnetizations of the two states. This is studied by comparing the results from DOS1 and DOS2. As shown in figure 3(c), the magnetization of the t_{2g} states relative to that of the e_g states $M(t_{2g})/M(e_g)$ is always larger for the result by DOS1. The relation between the results by DOS1 and DOS2 does not depend on U. In this case, thus, the character of the DOS at $E_{F,0}$ can be considered to mainly determine the result in figure 3(c). The relative intensities of the DOS projected onto the e_g and t_{2g} orbitals ($D_{e_g,0}(E_{F,0})$ and $D_{t_{2g},0}(E_{F,0})$) at $E_{F,0}$ explain the difference between the magnetization ratios $M(t_{2g})/M(e_g)$ by DOS1 and DOS2. As shown in figure 2, the intensity of the DOS projected onto the t_{2g} orbital relative to that onto the e_g orbital ($D_{t_{2g},0}(E_{F,0})/D_{e_g,0}(E_{F,0})$) is larger for DOS1 at $E_{F,0}$. This leads to a larger value of $M(t_{2g})/M(e_g)$ in the result using DOS1.

The magnetic behaviour of the e_g and t_{2g} states is expected to relate to the intra- and inter-orbital interactions in a systematic way, which can only be understood by using a multi-band model. Thus, the magnetizations of the two states are studied as functions of the Coulomb interaction U and the portion of the Hund's coupling J in the atomic interaction. An increase in J stabilizes the ferromagnetic solution and also affects the ratio between the magnetizations of the two states. In figure 4(a), showing the magnetization ratio as a function of the portion of J, the increase in the portion of J leads to the decrease in $M(t_{2g})/M(e_g)$. In doubly occupied configurations, the spin triplet states ($d_t^{\uparrow\uparrow}$, $d_t^{\downarrow\downarrow}$, d_t^0) stabilize with the increase in the portion of J (figure 4(b)), as shown in the energy of the atomic configuration (figure 1). Since the electron spins occupying the two orbitals align parallel in the spin triplet states, the increase in the portion of J results in a reduced difference between the magnetizations of the two states, which corresponds to the decrease in $M(t_{2g})/M(e_g)$ in this case (figure 4(a)). If the change of the magnetization ratio in figure 4(a) is viewed as a function of U, an increase in U is found to also bring about a decrease in $M(t_{2g})/M(e_g)$. As for the discussion on the magnetic behaviour by changing the portion of J, the probability of the spin triplet states is first evaluated as a function of U (figure 4(b)). Then, the probability of the spin triplet states surely increases in keeping with U in this electron

occupancy (figure 4(b)), since the energy difference among doubly occupied configurations is proportional to U and the energy of the spin triplet states is the lowest (figure 1). However, its dependence on U is weak compared to the probability change as a function of the portion of J. Further, the dependence of the probability of the spin triplet states on U weakens rather in the small portion of J, since the energy difference among doubly occupied configurations diminishes with the decrease in the portion of J. In this case, the dominant factor for the change in $M(t_{2g})/M(e_g)$ as a function of U can be considered to relate to the renormalized kinetic energy relative to U. The difference between the magnetizations of the two states originates from the kinetic energy part via the difference in the projected orbital DOS. The relative weight of the kinetic energy part in E^{var} is inversely proportional to U, owing to the atomic part proportional to U. Thus, if the difference between the renormalized kinetic energies of the $3d(e_g)$ and $3d(t_{2g})$ bands relative to U ($q_{e_g}\bar{\epsilon}_{e_g,0}/U$ and $q_{t_{2g}}\bar{\epsilon}_{t_{2g},0}/U$) reduces, the difference between the magnetizations of the two states decreases. The increase in U weakens the difference between $q_{e_g}\bar{\epsilon}_{e_g,0}/U$ and $q_{t_{2g}}\bar{\epsilon}_{t_{2g},0}/U$ and leads to a decrease in $M(t_{2g})/M(e_g)$ (figure 4(a)). These provide reasonable understanding for the systematic change of the magnetization ratio in figure 4(a). In this work, we have studied the magnetizations derived from the e_g and t_{2g} states as an important characteristic of the itinerant ferromagnetism by these states. The relative value of the magnetizations $M(t_{2g})/M(e_g)$ is found to be determined by the relative intensities of the projected orbital DOS at $E_{F,0}$, the stability of the spin triplet states, and the renormalized kinetic energies relative to U. The behaviour of the magnetizations by these factors is clarified by the analyses using the Gutzwiller variational method based on the two-band Hubbard model.

4. Summary

In this study, the ferromagnetism of the e_g and t_{2g} states has been investigated by the Gutzwiller variational method based on the two-band Hubbard model consisting of the e_g and t_{2g} states. In the previous work on the generalized Gutzwiller method [5], itinerant ferromagnetism in interacting multi-band systems was described by Gutzwiller wavefunctions using correlators for atomic eigenstates. Thus, its application to the specific case of the two degenerate e_g bands which have identical projected orbital DOSs showed that the stability of the atomic two-electron configurations consisting of the two e_g states influences the properties of the ferromagnetic phase such as the magnetization as a function of the Coulomb interaction U [5]. In this study, using the explicit form derived for the two states (e_g and t_{2g} states), the magnetizations of the e_g and t_{2g} states are examined. The result reproduces the feature that the magnetization shows a different value depending on the orbital. The difference (ratio) between the magnetizations by these states is discussed as characteristics of ferromagnetic phase derived from the two states that have different projected orbital DOSs. The factors determining the magnetizations of the e_g and t_{2g} states are summarized as the relative intensities of the projected orbital DOS at $E_{F,0}$, the renormalized kinetic energies relative to U, and the stability of the atomic configuration states. Thus, the stability of the atomic two-electron configurations consisting of the e_g and t_{2g} states also influences the ferromagnetic properties of this system as represented by the ratio between the magnetizations of the two states. The dependence of the magnetizations of the two states on the above factors has been investigated. The orbital-dependent magnetization is predominantly determined by the strength of the renormalization for each band, reflecting the spin-averaged kinetic energy of the uncorrelated case. Thus, the magnetization of the $3d(t_{2g})$ band renormalized more strongly has a larger value than that of the $3d(e_g)$ band. As expected, however, the detailed magnetization values are affected by the relative intensities of the DOS projected onto the two orbitals at $E_{F,0}$, which explains the change of the magnetization ratio $M(t_{2g})/M(e_g)$ accompanied by the difference in the DOS projected onto the two orbitals near $E_{F,0}$. The analysis as a function of the atomic interactions indicates that increases in the Coulomb interaction U and the portion of the Hund's coupling J in the atomic interaction bring about balanced magnetizations between the two states. The increase in U leads to a decrease in the renormalized kinetic energies relative to U and the increase in the portion of J stabilizes the spin triplet states. These features give a reasonable explanation for the magnetic behaviour as a function of the atomic interactions. Since the stabilization of the itinerant ferromagnetism requires large DOS at the Fermi energy, the Fermi surface is formed by the narrow $3d(e_g)$ and $3d(t_{2g})$ bands in 3d transition metals. Thus, the variation in the above factors can significantly affect the spin-dependent electronic structure near the Fermi energy.

References

[1] Stoner E C 1938 *Proc. R. Soc.* A **165** 372
[2] Kanamori J 1963 *Prog. Theor. Phys.* **30** 275
[3] Hubbard J 1963 *Proc. R. Soc.* A **276** 238
Hubbard J 1964 *Proc. R. Soc.* A **277** 237
Hubbard J 1964 *Proc. R. Soc.* A **281** 401
[4] Gutzwiller M C 1963 *Phys. Rev. Lett.* **10** 159
Gutzwiller M C 1964 *Phys. Rev.* **134** A923
Gutzwiller M C 1965 *Phys. Rev.* **137** A1726
[5] Bünemann J, Weber W and Gebhard F 1998 *Phys. Rev.* B **57** 6896
[6] Wang C S and Callaway J 1977 *Phys. Rev.* B **15** 298
[7] Himpsel F J, Knapp J A and Eastman D E 1979 *Phys. Rev.* B **19** 2919
[8] Eberhardt W and Plummer E W 1980 *Phys. Rev.* B **21** 3245
[9] Donath M 1994 *Surf. Sci. Rep.* **20** 251
[10] Biermann S, Aryasetiawan F and Georges A 2003 *Phys. Rev. Lett.* **90** 086402
[11] Bünemann J, Gebhard F, Ohm T, Weiser S and Weber W 2005 *Frontiers in Magnetic Materials* ed A Narlikar (Berlin: Springer)
[12] Kamakura N, Takata Y, Tokushima T, Harada Y, Chainani A, Kobayashi K and Shin S 2006 *Phys. Rev.* B **74** 045127
[13] Slater J C and Koster G F 1954 *Phys. Rev.* **94** 1498